



OPEN

Optical soliton solutions of the stochastic generalized nonlinear Schrödinger equation with arbitrary refractive index in Itô sense

Nafissa T. Trouba^{1,2}, Huiying Xu¹✉, Mohamed E. M. Alngar³✉, Reham M. A. Shohib⁴, Mohammed El-Meligy^{5,6}, Xinzhou Zhu^{1,7} & Mohamed Sharaf⁸

This paper introduce the stochastic generalized nonlinear Schrödinger equation (SGNLSE), which includes a stochastic term proportional to a Wiener process and models random refractive index variations in the Itô sense. This paper derives optical soliton solutions to the SGNLSE using the generalized Jacobi-elliptic function method. We investigate soliton solutions for $M = 1$, periodic wave solutions for $M = 0$, and Weierstrass elliptic function (WEF) solutions. The paper also discusses the physical implications of these solutions, particularly in the fields of nonlinear optics and plasma physics, where both stochastic perturbations and nonlinear effects significantly influence the dynamics of wave propagation. By exploring these solutions, this paper provides valuable insights into the combined effects of nonlinearity and randomness on wave propagation, which is important for understanding the behavior of complex systems where both deterministic and stochastic forces are at play.

Keywords Generalized nonlinear Schrödinger equation, Multiplicative noise, Stochastic soliton solutions, Generalized Jacobi-elliptic method

The nonlinear Schrödinger equation (NLSE) serves as a fundamental model in nonlinear science, describing diverse physical phenomena such as optical pulse propagation, matter-wave dynamics in Bose-Einstein condensates, and water waves. However, the classical NLSE often requires extensions to capture complex interactions and environmental effects. Among these extensions, the generalized nonlinear Schrödinger equation (GNLSE) introduces nonlinear dispersion and higher-order nonlinearities, allowing for the modeling of competing nonlinear effects and power-law dependencies on wave intensity^{1–11}.

In real-world scenarios, wave propagation often occurs in media with random fluctuations, such as varying refractive indices caused by thermal, quantum, or structural noise. To incorporate these effects, a stochastic term proportional to a Wiener process can be added to the GNLSE, resulting in the stochastic generalized nonlinear Schrödinger equation (SGNLSE). This stochastic term models an arbitrary refractive index in the Itô sense, introducing randomness into the wave dynamics and enabling the study of noise-induced phenomena^{12–22}.

The SGNLSE considered in this paper is given by:

$$iF_t - (|F|^{2m} F)_{xx} + [a|F|^{2n} + b|F|^{2p}]F + \delta F \frac{dW(t)}{dt} = 0, \quad m \neq -\frac{1}{2}. \quad (1)$$

¹School of Computer Science and Technology, Zhejiang Normal University, 321004 Jinhua, China. ²Zhejiang Institute of Photoelectronics, 321004 Jinhua, China. ³Mathematics Education Program, Faculty of Education and Arts, Sohar University, 311 Sohar, Oman. ⁴Basic Science Department, Higher Institute of Management Sciences & Foreign Trade, 379 Cairo, Egypt. ⁵Jadara University Research Center, Jadara University, PO Box 733 Irbid, Jordan. ⁶Applied Science Research Center, Applied Science Private University, Amman, Jordan. ⁷College of Computer Science and Artificial Intelligence, Wenzhou University, 325035 Wenzhou, China. ⁸Department of Industrial Engineering, College of Engineering, King Saud University, Riyadh 12372, Saudi Arabia. ✉email: xhy@zjnu.edu.cn; mohamed.alngar2010@yahoo.com

Equation (1) incorporates a multiplicative noise term represented by $\delta F \frac{dW(t)}{dt}$, where $W(t)$ is a standard Wiener process (Brownian motion) and δ is the noise strength. This term models random fluctuations in the refractive index of the propagation medium, such as those arising from thermal noise or structural imperfections. The equation is interpreted in the Itô sense, which is a standard framework in stochastic calculus for handling differential equations driven by noise. Unlike deterministic calculus, the Itô interpretation accounts for the non-differentiability of $W(t)$ and ensures well-defined integrals when the stochastic term is multiplicative (i.e., proportional to the solution F). This is particularly important in nonlinear optical systems, where noise interacts with the wave amplitude and phase in a nontrivial, intensity-dependent manner.

As a result, the SGNLSE in Eq. (1) captures both nonlinear deterministic dynamics and stochastic perturbations, enabling the exploration of noise-induced phenomena such as phase jitter, amplitude fluctuations, and soliton destabilization.

The function $F(x, t)$ is complex function, with t representing the temporal variable and x representing the spatial variable. The constants a and b are the parameters of Eq. (1), and $i^2 = -1$.

Equation (1) models the evolution of a soliton in a system where nonlinear dynamics and stochastic perturbations both play crucial roles. The equation represents a system where the deterministic part (without the stochastic term) governs the natural evolution of the wave, including nonlinear dispersion and intensity-dependent interactions. The stochastic term introduces random fluctuations that affect the wave's amplitude, phase, and propagation. This can be interpreted as random changes in the refractive index of the medium, such as those caused by thermal fluctuations, turbulence, or imperfections in the medium. The combination of these two effects makes the equation highly applicable in fields such as, nonlinear optics and plasma physics.

The Wiener process introduces fundamental randomness into the SGNLSE, which affects both the phase and amplitude of soliton solutions. Its statistical properties lead to diffusive effects and stochastic modulation, and the degree of soliton stability depends sensitively on the noise strength δ . Analyzing the propagation in terms of statistical averages and noise-induced thresholds becomes essential for realistic physical modeling. Ekici et al.⁶ explored exact soliton solutions for the deterministic NLSE with dual-power law nonlinearity using Jacobi elliptic function methods. Their results are particularly relevant since the nonlinear structure in their model is nearly identical to the nonlinear terms in our SGNLSE. The solutions derived in⁶ match the functional forms we obtain analytically in the noise-free limit ($\delta = 0$). However, Ekici et al. do not consider any stochastic contributions, and therefore do not account for noise-induced soliton deformation. Our inclusion of a stochastic term allows us to observe the progressive destabilization and decoherence of soliton solutions with increasing noise strength, an aspect not captured in the deterministic treatment of⁶. Consequently, our work can be viewed as a stochastic generalization of the models considered in⁶, bridging analytical theory and physical applicability in realistic settings where noise cannot be ignored.

Kudryashov⁷ investigated a generalized NLSE incorporating nonlinear dispersion and arbitrary refractive index, deriving exact stationary soliton solutions using an ansatz-based approach. The deterministic form of the equation studied in⁷ shares structural similarities with our SGNLSE when the stochastic term vanishes (i.e., $\delta = 0$). Both models involve competing nonlinear terms and support bright and dark soliton profiles. However, Kudryashov's model does not account for any stochastic effects. In contrast, our work extends the analysis by incorporating multiplicative white noise modeled by a Wiener process in the Itô sense. This stochastic component introduces amplitude fluctuations and phase jitter, which are absent in the deterministic framework of⁷, highlighting the physical relevance of our model in realistic noisy media such as optical fibers or plasma.

In earlier works, several generalizations of the nonlinear Schrödinger equation (NLSE) have been studied in deterministic settings. Kudryashov and Biswas⁸ investigated a generalized NLSE with two arbitrary refractive indices and obtained parametric solitary waves by applying transformations of dependent and independent variables. Kudryashov⁹ considered the family of NLSEs with unrestricted dispersion and polynomial nonlinearity, applying the Painlevé test and a new simplest-equation method to construct optical and embedded solitons. Further extensions were reported in¹⁰, where a triple-power law with non-local nonlinearity was introduced, leading to implicit solitary-wave solutions, while in¹¹ families of NLSEs with arbitrary functional forms were discussed, showing conditions under which generalized traveling waves exist. All these studies remain noise-free and focus on deterministic propagation models. By contrast, the present work develops a stochastic generalized NLSE with arbitrary refractive-index exponents in both the dispersive and nonlinear parts, together with a multiplicative Itô white-noise term modeling random refractive-index fluctuations. Through a traveling-wave reduction, we obtain an explicit Itô-corrected phase factor and a modified amplitude equation containing a δ^2 contribution. Using generalized Jacobi elliptic function expansions and Weierstrass functions, we construct bright, dark, periodic, and elliptic soliton solutions in closed form, together with explicit parameter constraints. Moreover, we analyze how the noise strength δ impacts soliton phase, amplitude, and stability, thereby extending deterministic catalogs of parametric solitons into the stochastic regime. This combination of arbitrary refractive-index laws with stochastic forcing and exact solution families represents the main novelty of the present study compared to^{6–11}.

The inclusion of an arbitrary refractive index in the SGNLSE is motivated by the need to describe nonlinear media whose dispersion and nonlinear response cannot be adequately captured by simple Kerr-type (integer power) laws. Such generalized refractive index profiles arise in a range of physical systems, including:

- Nonlinear optical fibers and photonic crystal fibers: Fabrication tolerances, dopant concentration gradients, and engineered microstructures can produce non-Kerr refractive index dependencies, leading to intensity-dependent dispersion and higher-order nonlinear effects.
- Plasma environments: Refractive index variations occur due to changes in plasma density, electron temperature, or external electromagnetic field modulation, often resulting in power-law or saturable nonlinearities.

- Bose–Einstein condensates (BECs): Effective refractive index analogues arise from atom-atom interaction strengths, which can be tuned via Feshbach resonances to produce non-standard nonlinear exponents.

The addition of a multiplicative noise term proportional to $\delta F \frac{dW(t)}{dt}$ reflects the reality that in many experimental systems, environmental fluctuations interact with the wave amplitude or intensity in a proportional manner rather than as purely additive noise. This is particularly relevant in:

- Optical fiber links: Random birefringence fluctuations, polarization mode dispersion, and thermally-induced refractive index changes scale with the optical field amplitude, leading to multiplicative stochastic modulation.
- High-power laser systems: Thermal lensing and gain medium inhomogeneities introduce noise whose strength depends on the local optical intensity.
- Plasma wave propagation: Density fluctuations or turbulence can modulate the refractive index in a manner proportional to the local wave amplitude.
- BEC experiments: Fluctuations in trapping potential or scattering length modulations due to noisy magnetic field control affect the condensate proportionally to its local density, thus manifesting as multiplicative noise.

The following experimental contexts demonstrate that the SGNLSE with arbitrary refractive index and multiplicative noise is not merely a mathematical abstraction, but a physically realizable model capable of describing complex nonlinear and noisy wave phenomena across multiple disciplines.

1. Dispersion-managed optical fibers with controlled refractive index profiles and thermal noise injection have been used to study soliton stability under stochastic perturbations, directly corresponding to the optical form of the SGNLSE.
2. Laser-plasma interaction chambers with externally driven density fluctuations provide a testbed for stochastic plasma wave models with arbitrary refractive index.
3. BEC waveguides with time-modulated Feshbach resonances allow precise control over both the effective nonlinearity exponent and the level of multiplicative noise via magnetic field noise engineering.

The purpose of this paper is to obtain analytical solutions to Eq. (1) using the generalized Jacobi-elliptic function method^{23,24}. We aim to derive Jacobi-elliptic function solutions, which include soliton solutions when $M = 1$, periodic wave solutions when $M = 0$, and the Weierstrass elliptic function (WEF) solutions.

Statistical role of the Wiener process in the SGNLSE

The Wiener process $W(t)$, also known as standard Brownian motion, is a fundamental stochastic process characterized by the following statistical properties:

- $W(0) = 0$ almost surely.
- For any $t > s$, the increment $W(t) - W(s)$ is normally distributed with mean zero and variance $t - s$, i.e., $W(t) - W(s) \sim \mathcal{N}(0, t - s)$.
- The increments are independent over non-overlapping intervals.
- Sample paths of $W(t)$ are almost surely continuous but nowhere differentiable. Consequently, the formal time derivative $\frac{dW(t)}{dt}$ is interpreted in the distributional sense as white noise.

In the context of the stochastic generalized nonlinear Schrödinger equation (SGNLSE), the inclusion of the multiplicative noise term $\delta F \frac{dW(t)}{dt}$ significantly alters the dynamics of soliton propagation. The main effects are:

- Phase Jitter: The stochastic phase modulation term $e^{i[\omega t + \delta W(t) - \delta^2 t]}$ introduces random fluctuations in the soliton phase. This leads to phase jitter that accumulates over time and degrades signal coherence, particularly in optical communication systems.
- Amplitude Fluctuations: The multiplicative nature of the noise causes the amplitude of the soliton to fluctuate stochastically. These fluctuations are more pronounced for higher values of δ , resulting in temporal or spatial deformation of the soliton profile.
- Reduced Stability: Solitons are inherently stable structures in deterministic nonlinear media, but the introduction of noise perturbs their balance. For weak noise ($\delta \ll 1$), solitons may persist with slight distortions. However, for strong noise ($\delta \gtrsim 1$), the soliton structure can break down entirely, leading to spreading, loss of localization, or chaotic dynamics.
- Statistical Soliton Description: Due to the randomness introduced by $W(t)$, deterministic descriptions become inadequate. Instead, ensemble averages such as the mean amplitude, soliton width variance, and mean squared displacement must be used to characterize the system. These quantities are essential for understanding propagation under realistic noisy conditions.
- Critical Noise Thresholds: There exists a critical noise strength δ_c beyond which the soliton loses coherence or ceases to exist. This threshold depends on initial conditions, nonlinearity parameters, and the physical context (e.g., optical fiber, plasma, or BEC).

Overall, the Wiener process introduces a rich layer of stochastic dynamics that profoundly affects soliton propagation. Understanding its statistical influence is crucial for designing robust nonlinear systems that operate under random environmental conditions.

This article is structured as follows: In Section 2, we present the mathematical analysis to derive the nonlinear ordinary differential equation (NLODE) corresponding to Eq. (1). In Section 3, we introduce the method for obtaining exact solutions to the NLODE. Section 4 provides the physical interpretation of the results. Finally, the conclusions are discussed in Section 5.

Mathematical analysis

In order to address this objective, we propose that the exact solution to Eq. (1) can be articulated in the subsequent manner:

$$F(x, t) = q(\zeta) e^{i[\kappa x + \omega t + \delta W(t) - \delta^2 t]}, \quad (2)$$

where $q(\zeta)$ represents real function and

$$\zeta = \beta x - vt. \quad (3)$$

For the physical definitions of all parameters, see Table 1.

Upon substituting Eqs. (2) and (3) into Eq. (1) and separating it into its real and imaginary components, we yield:

$$\begin{aligned} \Re : & (2m+1)\beta^2 q^{2m}(\zeta)q''(\zeta) + 2m(2m+1)\beta^2 q^{2m-1}(\zeta)q'^2(\zeta) - (2m+1)\beta\kappa^2 q^{2m}(\zeta)q'(\zeta) \\ & + (\delta^2 - \omega)q(\zeta) + aq^{2n+1}(\zeta) + bq^{2p+1}(\zeta) = 0, \end{aligned} \quad (4)$$

and

$$\Im : -vq'(\zeta) + \beta\kappa(2m+1)q^{2m}(\zeta)q'(\zeta) + (2m+1)\beta\kappa^2 [2mq^{2m-1}(\zeta)q'^2(\zeta) + q^{2m}(\zeta)q''(\zeta)] = 0. \quad (5)$$

Based on Equation (5), one can infer:

$$v = 0 \text{ and } \kappa = 0. \quad (6)$$

Consequently, Eq. (4) becomes:

$$(2m+1)\beta^2 q^{2m}(\zeta)q''(\zeta) + 2m(2m+1)\beta^2 q^{2m-1}(\zeta)q'^2(\zeta) + (\delta^2 - \omega)q(\zeta) + aq^{2n+1}(\zeta) + bq^{2p+1}(\zeta) = 0. \quad (7)$$

For performing the integration of Eq. (7), we should pick $p = 2m$ and $n = m$. In this case, Eq. (7) can be rewritten as

$$(2m+1)\beta^2 q^{2m}(\zeta)q''(\zeta) + 2m(2m+1)\beta^2 q^{2m-1}(\zeta)q'^2(\zeta) + (\delta^2 - \omega)q(\zeta) + aq^{2m+1}(\zeta) + bq^{4m+1}(\zeta) = 0. \quad (8)$$

To obtain solutions in a closed form, we consider the following transformation:

Symbol	Physical meaning and role in SGNLSE
$F(x, t)$	is the complex wave function representing the wave soliton. It evolves under the combined effects of dispersion, nonlinearity, and stochastic perturbations.
$ F ^{2m}, F ^{2n}$ and $ F ^{2p}$	represent nonlinear interactions between the wave function and its own intensity, and model intensity-dependent dispersion and refractive index behavior.
a	is the nonlinearity coefficient associated with the standard nonlinear term $a F ^{2n}F$. It governs self-phase modulation (SPM). A positive a induces focusing nonlinearity, while a negative a induces defocusing effects. Plays a central role in shaping soliton solutions.
b	is the coefficient of the higher-order nonlinear term $b F ^{2p}F$, used to model complex nonlinear behaviors such as multi-photon absorption or saturation effects. Influences the richness and diversity of exact solution structures.
δ	is the noise strength parameter for the multiplicative stochastic term $\delta F \frac{dW(t)}{dt}$. It determines the intensity of the stochastic influence on the wave, introducing amplitude fluctuations and phase jitter. Higher values lead to greater randomness in soliton behavior.
$W(t)$	is the Wiener process (Brownian motion), a stochastic process with independent Gaussian increments. Models environmental randomness such as thermal fluctuations or refractive-index disorder. Its derivative formally appears as white noise in the SGNLSE.
m	is power index of the nonlinear dispersion term $(F ^{2m}F)_{xx}$. It generalizes the dispersive behavior, allowing the equation to model intensity-dependent dispersion observed in certain optical media or plasmas.
n	is power index in the standard nonlinear term $a F ^{2n}F$. It generalizes the Kerr nonlinearity and determines the self-focusing/defocusing strength.
p	is power index in the higher-order nonlinear term $b F ^{2p}F$. Controls the degree and type of higher-order nonlinearity contributing to the wave dynamics.
β	is spatial scaling parameter introduced in the transformation $\zeta = \beta x - vt$, where ζ is a traveling coordinate. It controls the width and spatial frequency of the soliton and enables conversion of the SGNLSE into a solvable ordinary differential equation.
ω	is the temporal frequency term appearing in the solution's phase factor $e^{i[\omega t + \delta W(t) - \delta^2 t]}$. It governs the oscillatory time evolution of the soliton and couples with the noise to influence stability.

Table 1. Summary of parameters in the SGNLSE: physical meanings and roles.

$$q(\zeta) = [Q(\zeta)]^{\frac{1}{m}}, \quad (9)$$

provided $Q(\zeta) > 0$. By substituting Eq. (9) into Eq. (8), we obtain:

$$m(2m+1)\beta^2 Q(\zeta)Q''(\zeta) + (m+1)(2m+1)\beta^2 Q'^2(\zeta) + m^2 (\delta^2 - \omega) + am^2 Q^2(\zeta) + bm^2 Q^4(\zeta) = 0. \quad (10)$$

Generalized Jacobi-elliptic function method

We assume that Eq. (10) has the formal solution:

$$Q(\zeta) = \Xi_0 + \sum_{l=1}^N \Xi_l \Theta^l(\zeta). \quad (11)$$

Here, $N \in \mathbb{Z}^+$, and Ξ_l for ($l = 0, 1, \dots, N$) represent constants, given that $\Xi_N \neq 0$. Additionally, $\Theta(\zeta)$ denotes the solution to:

$$\Theta'(\zeta) = \sqrt{g_0 + g_2 \Theta^2(\zeta) + g_4 \Theta^4(\zeta)}. \quad (12)$$

Here g_0, g_2 and g_4 are constants. It is commonly acknowledged^{23,24}, that Eq. (12) allows for the following solutions:

Family-1: If $\chi = \frac{g_2}{g_4} \chi$, then one gets the generalized Jacobi-elliptic function solutions (JEFs):

Set-1. If $\chi = \frac{M^2(M^2 - 1)}{2M^2 - 1}$, $0 < M < 1$, then:

$$\Theta(\zeta) = \begin{cases} \pm M \sqrt{-\frac{g_2}{(2M^2 - 1)g_4}} \operatorname{cn} \left(\sqrt{\frac{g_2}{2M^2 - 1}} \zeta \right), & (2M^2 - 1)g_2 > 0, g_4 < 0, \\ \pm \sqrt{\frac{(1 - M^2)g_2}{(2M^2 - 1)g_4}} \operatorname{nc} \left(\sqrt{\frac{g_2}{2M^2 - 1}} \zeta \right), & (2M^2 - 1)g_2 > 0, g_4 > 0, \\ \pm M \sqrt{-\frac{(1 - M^2)g_2}{(2M^2 - 1)g_4}} \operatorname{sd} \left(\sqrt{\frac{g_2}{2M^2 - 1}} \zeta \right), & (2M^2 - 1)g_2 > 0, g_4 < 0, \\ \pm \sqrt{\frac{g_2}{(2M^2 - 1)g_4}} \operatorname{ds} \left(\sqrt{\frac{g_2}{2M^2 - 1}} \zeta \right), & (2M^2 - 1)g_2 > 0, g_4 > 0. \end{cases} \quad (13)$$

Set-2. If $\chi = \frac{M^2}{(1 + M^2)^2}$, $0 < M < 1$, then:

$$\Theta(\zeta) = \begin{cases} \pm M \sqrt{-\frac{g_2}{(1 + M^2)g_4}} \operatorname{sn} \left(\sqrt{-\frac{g_2}{1 + M^2}} \zeta \right), & g_2 < 0, g_4 > 0, \\ \pm \sqrt{-\frac{g_2}{(1 + M^2)g_4}} \operatorname{ns} \left(\sqrt{-\frac{g_2}{1 + M^2}} \zeta \right), & g_2 < 0, g_4 > 0, \\ \pm M \sqrt{-\frac{g_2}{(1 + M^2)g_4}} \operatorname{cd} \left(\sqrt{-\frac{g_2}{1 + M^2}} \zeta \right), & g_2 < 0, g_4 > 0, \\ \pm \sqrt{-\frac{g_2}{(1 + M^2)g_4}} \operatorname{dc} \left(\sqrt{-\frac{g_2}{1 + M^2}} \zeta \right), & g_2 < 0, g_4 > 0. \end{cases} \quad (14)$$

Set-3. If $\chi = \frac{(1 - M^2)}{(2 - M^2)^2}$, $0 < M < 1$, then:

$$\Theta(\zeta) = \begin{cases} \pm \sqrt{-\frac{g_2}{(2 - M^2)g_4}} \operatorname{dn} \left(\sqrt{\frac{g_2}{2 - M^2}} \zeta \right), & g_2 > 0, g_4 < 0, \\ \pm \sqrt{-\frac{(1 - M^2)g_2}{(2 - M^2)g_4}} \operatorname{nd} \left(\sqrt{\frac{g_2}{2 - M^2}} \zeta \right), & g_2 > 0, g_4 < 0, \\ \pm \sqrt{\frac{g_2}{(2 - M^2)g_4}} \operatorname{cs} \left(\sqrt{\frac{g_2}{2 - M^2}} \zeta \right), & g_2 > 0, g_4 > 0, \\ \pm \sqrt{\frac{(1 - M^2)g_2}{(2 - M^2)g_4}} \operatorname{sc} \left(\sqrt{\frac{g_2}{2 - M^2}} \zeta \right), & g_2 > 0, g_4 > 0. \end{cases} \quad (15)$$

Set-4. If $\chi = \frac{(1 - M^2)^2}{4(1 + M^2)^2}$, $0 < M < 1$, then:

$$\Theta(\zeta) = \begin{cases} \pm \sqrt{-\frac{g_2}{2(1+M^2)g_4}} \left[M \operatorname{cn} \left(\sqrt{\frac{2g_2}{1+M^2}} \zeta \right) \pm \operatorname{dn} \left(\sqrt{\frac{2g_2}{1+M^2}} \zeta \right) \right], & g_2 > 0, g_4 < 0, \\ \pm \sqrt{-\frac{(1-M^2)g_2}{2(1+M^2)g_4}} \left[M \operatorname{sd} \left(\sqrt{\frac{2g_2}{1+M^2}} \zeta \right) \pm \operatorname{nd} \left(\sqrt{\frac{2g_2}{1+M^2}} \zeta \right) \right], & g_2 > 0, g_4 < 0, \\ \pm \sqrt{\frac{(1-M^2)g_2}{2(1+M^2)g_4}} \left[\operatorname{nc} \left(\sqrt{\frac{2g_2}{1+M^2}} \zeta \right) \pm \operatorname{sc} \left(\sqrt{\frac{2g_2}{1+M^2}} \zeta \right) \right], & g_2 > 0, g_4 > 0, \\ \pm \sqrt{\frac{g_2}{2(1+M^2)g_4}} \left[\operatorname{ds} \left(\sqrt{\frac{2g_2}{1+M^2}} \zeta \right) \pm \operatorname{cs} \left(\sqrt{\frac{2g_2}{1+M^2}} \zeta \right) \right], & g_2 > 0, g_4 > 0, \\ \pm \sqrt{\frac{(1-M^2)g_2}{2(1+M^2)g_4}} \operatorname{cn} \left(\sqrt{\frac{2g_2}{1+M^2}} \zeta \right) \left[1 \pm \operatorname{sn} \left(\sqrt{\frac{2g_2}{1+M^2}} \zeta \right) \right]^{-1}, & g_2 > 0, g_4 > 0. \end{cases} \quad (16)$$

Set-5. If $\chi = \frac{M^4}{4(2-M^2)^2}$, $0 < M < 1$, then:

$$\Theta(\zeta) = \begin{cases} \pm \sqrt{-\frac{g_2}{2(2-M^2)g_4}} \left[\sqrt{1-M^2} \operatorname{nc} \left(\sqrt{-\frac{2g_2}{2-M^2}} \zeta \right) \pm \operatorname{dc} \left(\sqrt{-\frac{2g_2}{2-M^2}} \zeta \right) \right], & g_2 < 0, g_4 > 0, \\ \pm \sqrt{-\frac{g_2}{2(2-M^2)g_4}} \left[\operatorname{ns} \left(\sqrt{-\frac{2g_2}{2-M^2}} \zeta \right) \pm \operatorname{ds} \left(\sqrt{-\frac{2g_2}{2-M^2}} \zeta \right) \right], & g_2 < 0, g_4 > 0, \\ \pm M \sqrt{-\frac{g_2}{2(2-M^2)g_4}} \left[\operatorname{sn} \left(\sqrt{-\frac{2g_2}{2-M^2}} \zeta \right) \pm i \operatorname{cn} \left(\sqrt{-\frac{2g_2}{2-M^2}} \zeta \right) \right], & g_2 < 0, g_4 > 0. \end{cases} \quad (17)$$

Set-6. If $\chi = \frac{1}{4(1-2M^2)^2}$, $0 < M < 1$, then:

$$\Theta(\zeta) = \begin{cases} \pm \sqrt{\frac{g_2}{2(1-2M^2)g_4}} \left[M \operatorname{sn} \left(\sqrt{\frac{2g_2}{1-2M^2}} \zeta \right) \pm i \operatorname{dn} \left(\sqrt{\frac{2g_2}{1-2M^2}} \zeta \right) \right], & (1-2M^2)g_2 > 0, g_4 > 0, \\ \pm \sqrt{\frac{g_2}{2(1-2M^2)g_4}} \left[\operatorname{ns} \left(\sqrt{\frac{2g_2}{1-2M^2}} \zeta \right) \pm \operatorname{cs} \left(\sqrt{\frac{2g_2}{1-2M^2}} \zeta \right) \right], & (1-2M^2)g_2 > 0, g_4 > 0, \\ \pm \sqrt{\frac{g_2}{2(1-2M^2)g_4}} \left[\sqrt{1-M^2} \operatorname{sc} \left(\sqrt{\frac{2g_2}{1-2M^2}} \zeta \right) \pm \operatorname{dc} \left(\sqrt{\frac{2g_2}{1-2M^2}} \zeta \right) \right], & (1-2M^2)g_2 > 0, g_4 > 0. \end{cases} \quad (18)$$

Family-2: Equation (12) has the solutions in terms of Weierstrass elliptic function (WEF) solutions:
Type-1:

$$\Theta(\zeta) = \begin{cases} \frac{3\wp'(\zeta, r_2, r_3)}{\sqrt{g_4}[6\wp(\zeta, r_2, r_3) + g_2]}, & g_4 > 0, \\ \frac{\sqrt{g_4}[6\wp(\zeta, r_2, r_3) + g_2]}{\sqrt{g_0}[6\wp(\zeta, r_2, r_3) + g_2]}, & g_0 > 0, \\ \frac{3\wp'(\zeta, r_2, r_3)}{3\wp(\zeta, r_2, r_3)}, & \text{otherwise} \end{cases} \quad (19)$$

where

$$r_2 = g_0g_4 + \frac{g_2}{12} \text{ and } r_3 = \frac{g_2(36g_0g_4 - g_2)}{216}. \quad (20)$$

Type-2:

$$\Theta(\zeta) = \begin{cases} \sqrt{\frac{3\wp(\zeta, r_2, r_3) - g_2}{3g_4}}, \\ \sqrt{\frac{3g_0}{3\wp(\zeta, r_2, r_3) - g_2}}, \end{cases} \quad (21)$$

where

$$r_2 = \frac{4}{3}g_2 - 3g_0g_4 \text{ and } r_3 = \frac{4}{27}(9g_0g_2g_4 - 2g_2). \quad (22)$$

In this context, $\wp(\zeta, r_2, r_3)$ denotes a WEF, and $\wp'(\zeta, r_2, r_3) = \frac{d\wp(\zeta, r_2, r_3)}{dz}$, which satisfies the equation: $\wp'^2 = 4\wp^3 - r_2\wp - r_3$, where r_2 and r_3 are referred to as the invariants of the WEF.

Optical solitons

We balance $Q(\zeta)Q''(\zeta)$ and $Q^4(\zeta)$ in Eq. (10), we get $N = 1$, thus, the solution of Eq. (10) has the solution:

$$Q(\zeta) = \Xi_0 + \Xi_1 \Theta(\zeta). \quad (23)$$

Substituting (23) and (12) into (10), we derive the resulting set of algebraic equations:

$$\left. \begin{aligned} \Xi_1^2 & \left[(b\Xi_1^2 + 6g_4\beta^2)m^2 + 5m\beta^2g_4 + g_4\beta^2 \right] = 0, \\ 4m\Xi_1\Xi_0 & \left[2(b\Xi_1^2 + g_4\beta^2)m + g_4\beta^2 \right] = 0, \\ \Xi_1^2 & \left[(a + 6b\Xi_0^2 + 4g_2\beta^2)m^2 + (4m + 1)\beta^2g_2 \right] = 0, \\ m\Xi_0\Xi_1 & \left[2(2b\Xi_0^2 + g_2\beta^2 + a) + g_2\beta^2 \right] = 0, \\ m^2(a\Xi_0^2 + b\Xi_0^4 + \delta^2 - \omega) & + (2m^2 + 3m + 1)\Xi_1^2g_0\beta^2 = 0. \end{aligned} \right\} \quad (24)$$

Result-1: Set $g_0 = \frac{g_2^4}{g_4}\chi$, in Eq. (24), and solve it, one gets the results:

$$\Xi_0 = 0, \quad \Xi_1 = \pm \frac{\beta}{m} \sqrt{-\frac{(6m^2 + 5m + 1)g_4}{b}}, \quad g_2 = -\frac{m^2a}{(2m + 1)^2\beta^2}, \quad (25)$$

and

$$\omega = \delta^2 - \frac{(m + 1)(3m + 1)a^2}{(2m + 1)^2b}\chi. \quad (26)$$

By substituting (25) along with (13)–(18) into (23), it follows the following solutions:

Case-1. If $\chi = \frac{M^2(M^2 - 1)}{(2M^2 - 1)}$, then Eq. (1) has the JEFs as:

$$F(x, t) = \left[\pm \frac{M}{2m + 1} \sqrt{-\frac{a(6m^2 + 5m + 1)}{b(2M^2 - 1)}} \operatorname{cn} \left(\frac{m}{2m + 1} \sqrt{-\frac{a}{2M^2 - 1}}x, M \right) \right]^{\frac{1}{m}} e^{i[\omega t + \delta W(t) - \delta^2 t]}, \quad (27)$$

$$F(x, t) = \left[\pm \frac{M}{2m + 1} \sqrt{-\frac{a(6m^2 + 5m + 1)(1 - M^2)}{b(2M^2 - 1)}} \operatorname{sd} \left(\frac{m}{2m + 1} \sqrt{-\frac{a}{2M^2 - 1}}x, M \right) \right]^{\frac{1}{m}} e^{i[\omega t + \delta W(t) - \delta^2 t]}, \quad (28)$$

provided $(2M^2 - 1)a < 0$, $(6m^2 + 5m + 1)b > 0$, and

$$F(x, t) = \left[\pm \frac{1}{2m + 1} \sqrt{\frac{a(6m^2 + 5m + 1)(1 - M^2)}{b(2M^2 - 1)}} \operatorname{nc} \left(\frac{m}{2m + 1} \sqrt{-\frac{a}{2M^2 - 1}}x, M \right) \right]^{\frac{1}{m}} e^{i[\omega t + \delta W(t) - \delta^2 t]}, \quad (29)$$

$$F(x, t) = \left[\pm \frac{1}{2m + 1} \sqrt{\frac{a(6m^2 + 5m + 1)}{b(2M^2 - 1)}} \operatorname{ds} \left(\frac{m}{2m + 1} \sqrt{-\frac{a}{2M^2 - 1}}x, M \right) \right]^{\frac{1}{m}} e^{i[\omega t + \delta W(t) - \delta^2 t]}, \quad (30)$$

provided $(2M^2 - 1)a < 0$ and $(6m^2 + 5m + 1)b < 0$.

When $M = 1$ in Eqs. (27) and (30), it results, respectively in the bright soliton solution:

$$F(x, t) = \left[\pm \frac{1}{2m + 1} \sqrt{-\frac{a(6m^2 + 5m + 1)}{b}} \operatorname{sech} \left(\frac{m\sqrt{-a}}{2m + 1}x \right) \right]^{\frac{1}{m}} e^{i[\omega t + \delta W(t) - \delta^2 t]}, \quad (31)$$

provided $a < 0$ and $(6m^2 + 5m + 1)b > 0$, and the singular soliton solution:

$$F(x, t) = \left[\pm \frac{1}{2m + 1} \sqrt{\frac{a(6m^2 + 5m + 1)}{b}} \operatorname{csch} \left(\frac{m\sqrt{-a}}{2m + 1}x \right) \right]^{\frac{1}{m}} e^{i[\omega t + \delta W(t) - \delta^2 t]}, \quad (32)$$

provided $a < 0$ and $(6m^2 + 5m + 1)b < 0$.

While, if $M = 0$ in Eqs. (29) and (30), it results, respectively the periodic wave solutions:

$$F(x, t) = \left[\pm \frac{1}{2m + 1} \sqrt{-\frac{a(6m^2 + 5m + 1)}{b}} \operatorname{sec} \left(\frac{m\sqrt{a}}{2m + 1}x \right) \right]^{\frac{1}{m}} e^{i[\omega t + \delta W(t) - \delta^2 t]}, \quad (33)$$

and

$$F(x, t) = \left[\pm \frac{1}{2m+1} \sqrt{-\frac{a(6m^2 + 5m + 1)}{b}} \csc \left(\frac{m\sqrt{a}}{2m+1} x \right) \right]^{\frac{1}{m}} e^{i[\omega t + \delta W(t) - \delta^2 t]}, \quad (34)$$

provided $a > 0$ and $(6m^2 + 5m + 1)b < 0$.

Remark 1 Due to the translational invariance of the stochastic generalized nonlinear Schrödinger equation, each analytical solution admits arbitrary spatial and temporal shifts, $\zeta \rightarrow \zeta - \zeta_0$, $t \rightarrow t - t_0$, where ζ_0 and t_0 are real constants determined by the initial or boundary conditions. For compactness, these constants are set to zero in the expressions presented here, without loss of generality.

Case-2. If $\chi = \frac{M^2}{(1 + M^2)^2}$, then Eq. (1) has the JEFs as:

$$F(x, t) = \left[\pm \frac{M}{2m+1} \sqrt{-\frac{a(6m^2 + 5m + 1)}{b(1 + M^2)}} \operatorname{sn} \left(\frac{m}{2m+1} \sqrt{\frac{a}{1 + M^2}} x, M \right) \right]^{\frac{1}{m}} e^{i[\omega t + \delta W(t) - \delta^2 t]}, \quad (35)$$

$$F(x, t) = \left[\pm \frac{1}{2m+1} \sqrt{-\frac{a(6m^2 + 5m + 1)}{b(1 + M^2)}} \operatorname{ns} \left(\frac{m}{2m+1} \sqrt{\frac{a}{1 + M^2}} x, M \right) \right]^{\frac{1}{m}} e^{i[\omega t + \delta W(t) - \delta^2 t]}, \quad (36)$$

$$F(x, t) = \left[\pm \frac{M}{2m+1} \sqrt{-\frac{a(6m^2 + 5m + 1)}{b(1 + M^2)}} \operatorname{cd} \left(\frac{m}{2m+1} \sqrt{\frac{a}{1 + M^2}} x, M \right) \right]^{\frac{1}{m}} e^{i[\omega t + \delta W(t) - \delta^2 t]}, \quad (37)$$

$$F(x, t) = \left[\pm \frac{1}{2m+1} \sqrt{-\frac{a(6m^2 + 5m + 1)}{b(1 + M^2)}} \operatorname{dc} \left(\frac{m}{2m+1} \sqrt{\frac{a}{1 + M^2}} x, M \right) \right]^{\frac{1}{m}} e^{i[\omega t + \delta W(t) - \delta^2 t]}, \quad (38)$$

provided $a > 0$ and $(6m^2 + 5m + 1)b < 0$.

When $M = 1$ in Eqs. (35) and (36), it results, respectively in the dark soliton solution:

$$F(x, t) = \left[\pm \frac{1}{2m+1} \sqrt{-\frac{a(6m^2 + 5m + 1)}{2b}} \tanh \left(\frac{m}{2m+1} \sqrt{\frac{a}{2}} x \right) \right]^{\frac{1}{m}} e^{i[\omega t + \delta W(t) - \delta^2 t]}, \quad (39)$$

and the singular soliton solution:

$$F(x, t) = \left[\pm \frac{1}{2m+1} \sqrt{-\frac{a(6m^2 + 5m + 1)}{2b}} \coth \left(\frac{m}{2m+1} \sqrt{\frac{a}{2}} x \right) \right]^{\frac{1}{m}} e^{i[\omega t + \delta W(t) - \delta^2 t]}, \quad (40)$$

provided $a > 0$ and $(6m^2 + 5m + 1)b < 0$.

Case-3. If $\chi = \frac{(1 - M^2)}{(2 - M^2)^2}$, then Eq. (1) has the JEFs as:

$$F(x, t) = \left[\pm \frac{1}{2m+1} \sqrt{-\frac{a(6m^2 + 5m + 1)}{b(2 - M^2)}} \operatorname{dn} \left(\frac{m}{2m+1} \sqrt{-\frac{a}{2 - M^2}} x, M \right) \right]^{\frac{1}{m}} e^{i[\omega t + \delta W(t) - \delta^2 t]}, \quad (41)$$

$$F(x, t) = \left[\pm \frac{1}{2m+1} \sqrt{-\frac{a(6m^2 + 5m + 1)(1 - M^2)}{b(2 - M^2)}} \operatorname{nd} \left(\frac{m}{2m+1} \sqrt{-\frac{a}{2 - M^2}} x, M \right) \right]^{\frac{1}{m}} e^{i[\omega t + \delta W(t) - \delta^2 t]}, \quad (42)$$

$$F(x, t) = \left[\pm \frac{1}{2m+1} \sqrt{-\frac{a(6m^2 + 5m + 1)}{b(2 - M^2)}} \operatorname{cs} \left(\frac{m}{2m+1} \sqrt{-\frac{a}{2 - M^2}} x, M \right) \right]^{\frac{1}{m}} e^{i[\omega t + \delta W(t) - \delta^2 t]}, \quad (43)$$

$$F(x, t) = \left[\pm \frac{1}{2m+1} \sqrt{-\frac{a(6m^2 + 5m + 1)(1 - M^2)}{b(2 - M^2)}} \operatorname{sc} \left(\frac{m}{2m+1} \sqrt{-\frac{a}{2 - M^2}} x, M \right) \right]^{\frac{1}{m}} e^{i[\omega t + \delta W(t) - \delta^2 t]}, \quad (44)$$

provided $a < 0$ and $(6m^2 + 5m + 1)b > 0$.

When $M = 0$ in Eqs. (43) and (44), it results, respectively in the periodic wave solutions:

$$F(x, t) = \left[\pm \frac{1}{2m+1} \sqrt{-\frac{a(6m^2 + 5m + 1)}{2b}} \cot \left(\frac{m}{2m+1} \sqrt{-\frac{a}{2}} x \right) \right]^{\frac{1}{m}} e^{i[\omega t + \delta W(t) - \delta^2 t]}, \quad (45)$$

and

$$F(x, t) = \left[\pm \frac{1}{2m+1} \sqrt{-\frac{a(6m^2 + 5m + 1)}{2b}} \tan \left(\frac{m}{2m+1} \sqrt{-\frac{a}{2}} x \right) \right]^{\frac{1}{m}} e^{i[\omega t + \delta W(t) - \delta^2 t]}, \quad (46)$$

provided $a < 0$ and $(6m^2 + 5m + 1)b > 0$.

Case-4. If $\chi = \frac{(1 - M^2)^2}{4(1 + M^2)^2}$, then Eq. (1) has the JEFs as:

$$F(x, t) = \left[\pm \frac{1}{2m+1} \sqrt{-\frac{a(6m^2 + 5m + 1)}{2b(1 + M^2)}} \left\{ M \operatorname{cn} \left(\frac{m}{2m+1} \sqrt{-\frac{2a}{1+M^2}} x, M \right) + \operatorname{dn} \left(\frac{m}{2m+1} \sqrt{-\frac{2a}{1+M^2}} x, M \right) \right\} \right]^{\frac{1}{m}} e^{i[\omega t + \delta W(t) - \delta^2 t]}, \quad (47)$$

$$F(x, t) = \left[\pm \frac{1}{2m+1} \sqrt{-\frac{a(6m^2 + 5m + 1)(1 - M^2)}{2b(1 + M^2)}} \left\{ M \operatorname{sd} \left(\frac{m}{2m+1} \sqrt{-\frac{2a}{1+M^2}} x, M \right) + \operatorname{nd} \left(\frac{m}{2m+1} \sqrt{-\frac{2a}{1+M^2}} x, M \right) \right\} \right]^{\frac{1}{m}} e^{i[\omega t + \delta W(t) - \delta^2 t]}, \quad (48)$$

provided $a < 0$ and $(6m^2 + 5m + 1)b > 0$.

$$F(x, t) = \left[\pm \frac{1}{2m+1} \sqrt{\frac{a(6m^2 + 5m + 1)(1 - M^2)}{2b(1 + M^2)}} \left\{ \operatorname{nc} \left(\frac{m}{2m+1} \sqrt{-\frac{2a}{1+M^2}} x, M \right) + \operatorname{sc} \left(\frac{m}{2m+1} \sqrt{-\frac{2a}{1+M^2}} x, M \right) \right\} \right]^{\frac{1}{m}} e^{i[\omega t + \delta W(t) - \delta^2 t]}, \quad (49)$$

$$F(x, t) = \left[\pm \frac{1}{2m+1} \sqrt{\frac{a(6m^2 + 5m + 1)}{2b(1 + M^2)}} \left\{ \operatorname{ds} \left(\frac{m}{2m+1} \sqrt{-\frac{2a}{1+M^2}} x, M \right) + \operatorname{cs} \left(\frac{m}{2m+1} \sqrt{-\frac{2a}{1+M^2}} x, M \right) \right\} \right]^{\frac{1}{m}} e^{i[\omega t + \delta W(t) - \delta^2 t]}, \quad (50)$$

$$F(x, t) = \left[\pm \frac{1}{2m+1} \sqrt{\frac{a(6m^2 + 5m + 1)(1 - M^2)}{2b(1 + M^2)}} \left\{ \frac{\operatorname{cn} \left(\frac{m}{2m+1} \sqrt{-\frac{2a}{1+M^2}} x, M \right)}{1 + \operatorname{sn} \left(\frac{m}{2m+1} \sqrt{-\frac{2a}{1+M^2}} x, M \right)} \right\} \right]^{\frac{1}{m}} e^{i[\omega t + \delta W(t) - \delta^2 t]}, \quad (51)$$

provided $a < 0$ and $(6m^2 + 5m + 1)b < 0$.

When $M = 0$ in Eqs. (49)–(51), it results, respectively in the periodic wave solutions:

$$F(x, t) = \left[\pm \frac{1}{2m+1} \sqrt{\frac{a(6m^2 + 5m + 1)}{2b}} \left\{ \sec \left(\frac{m\sqrt{-2a}}{2m+1} x \right) + \tan \left(\frac{m\sqrt{-2a}}{2m+1} x \right) \right\} \right]^{\frac{1}{m}} e^{i[\omega t + \delta W(t) - \delta^2 t]}, \quad (52)$$

$$F(x, t) = \left[\pm \frac{1}{2m+1} \sqrt{\frac{a(6m^2 + 5m + 1)}{2b}} \left\{ \csc \left(\frac{m\sqrt{-2a}}{2m+1} x \right) + \cot \left(\frac{m\sqrt{-2a}}{2m+1} x \right) \right\} \right]^{\frac{1}{m}} e^{i[\omega t + \delta W(t) - \delta^2 t]}, \quad (53)$$

$$F(x, t) = \left[\pm \frac{1}{2m+1} \sqrt{\frac{a(6m^2 + 5m + 1)}{2b}} \left\{ \frac{\cos \left(\frac{m}{2m+1} \sqrt{-2ax} \right)}{1 + \sin \left(\frac{m}{2m+1} \sqrt{-2ax} \right)} \right\} \right]^{\frac{1}{m}} e^{i[\omega t + \delta W(t) - \delta^2 t]}, \quad (54)$$

provided $a < 0$ and $(6m^2 + 5m + 1)b < 0$.

Case-5. If $\chi = \frac{M^4}{4(2 - M^2)^2}$, then Eq. (1) has the JEFs as:

$$F(x, t) = \left[\pm \frac{1}{2m+1} \sqrt{-\frac{a(6m^2 + 5m + 1)}{2b(2 - M^2)}} \left\{ \sqrt{1 - M^2} \operatorname{nc} \left(\frac{m}{2m+1} \sqrt{\frac{2a}{2-M^2}} x, M \right) + \operatorname{dc} \left(\frac{m}{2m+1} \sqrt{\frac{2a}{2-M^2}} x, M \right) \right\} \right]^{\frac{1}{m}} e^{i[\omega t + \delta W(t) - \delta^2 t]}, \quad (55)$$

$$F(x, t) = \left[\pm \frac{1}{2m+1} \sqrt{-\frac{a(6m^2 + 5m + 1)}{2b(2 - M^2)}} \left\{ \operatorname{ns} \left(\frac{m}{2m+1} \sqrt{\frac{2a}{2-M^2}} x, M \right) + \operatorname{ds} \left(\frac{m}{2m+1} \sqrt{\frac{2a}{2-M^2}} x, M \right) \right\} \right]^{\frac{1}{m}} e^{i[\omega t + \delta W(t) - \delta^2 t]}, \quad (56)$$

provided $a > 0$ and $(6m^2 + 5m + 1)b < 0$.

When $M = 1$ in Eq. (56), it results, the combo-singular soliton solution:

$$F(x, t) = \left[\pm \frac{1}{2m+1} \sqrt{-\frac{a(6m^2 + 5m + 1)}{2b}} \left\{ \operatorname{csch} \left(\frac{m\sqrt{2a}}{2m+1} x \right) + \operatorname{coth} \left(\frac{m\sqrt{2a}}{2m+1} x \right) \right\} \right]^{\frac{1}{m}} e^{i[\omega t + \delta W(t) - \delta^2 t]}, \quad (57)$$

provided $a > 0$ and $(6m^2 + 5m + 1)b < 0$.

Case-6. If $\chi = \frac{1}{4(1-2M^2)^2}$, then Eq. (1) has the JEFs as:

$$F(x, t) = \left[\pm \frac{1}{2m+1} \sqrt{\frac{a(6m^2 + 5m + 1)}{2b(1-2M^2)}} \left\{ \operatorname{ns} \left(\frac{m}{2m+1} \sqrt{-\frac{2a}{1-2M^2}} x, M \right) + \operatorname{cs} \left(\frac{m}{2m+1} \sqrt{-\frac{2a}{1-2M^2}} x, M \right) \right\} \right]^{\frac{1}{m}} e^{i[\omega t + \delta W(t) - \delta^2 t]}, \quad (58)$$

$$F(x, t) = \left[\pm \frac{1}{2m+1} \sqrt{\frac{a(6m^2 + 5m + 1)}{2b(1-2M^2)}} \left\{ \sqrt{1-M^2} \operatorname{sc} \left(\frac{m}{2m+1} \sqrt{-\frac{2a}{1-2M^2}} x, M \right) + \operatorname{dc} \left(\frac{m}{2m+1} \sqrt{-\frac{2a}{1-2M^2}} x, M \right) \right\} \right]^{\frac{1}{m}} e^{i[\omega t + \delta W(t) - \delta^2 t]}, \quad (59)$$

provided $a(1-2M^2) < 0$ and $(6m^2 + 5m + 1)b < 0$.

Result-2. On solving Eq. (24) with Maple, one gets:

$$\Xi_0 = 0, \Xi_1 = \pm \frac{\beta}{m} \sqrt{-\frac{(6m^2 + 5m + 1)g_4}{b}}, g_0 = -\frac{bm^4(\omega - \sigma^2)}{g_4\beta^4(12m^4 + 28m^3 + 23m^2 + 8m + 1)}, g_2 = -\frac{m^2a}{(2m+1)^2\beta^2}, \quad (60)$$

provided $(6m^2 + 5m + 1)bg_4 < 0$. By incorporating (69) in conjunction with (19) and (21) into (23), it follows that Eq. (1) present:

(I) The Weierstrass elliptic function solutions as:

$$F(x, t) = \left[\pm \frac{3\beta}{m} \sqrt{-\frac{6m^2 + 5m + 1}{b}} \left(\frac{\wp'(\beta x, r_2, r_3)}{6\wp(\beta x, r_2, r_3) - \frac{am^2}{\beta^2(2m+1)^2}} \right) \right]^{\frac{1}{m}} e^{i[\omega t + \delta W(t) - \delta^2 t]}, \quad (61)$$

provided $(6m^2 + 5m + 1)b < 0$, and

$$F(x, t) = \left[\pm \frac{m}{3\beta} \sqrt{\frac{(6m^2 + 5m + 1)(\omega - \sigma^2)}{(12m^4 + 28m^3 + 23m^2 + 8m + 1)}} \left(\frac{6\wp(\beta x, r_2, r_3) - \frac{am^2}{\beta^2(2m+1)^2}}{m\wp'(\beta x, r_2, r_3)} \right) \right]^{\frac{1}{m}} e^{i[\omega t + \delta W(t) - \delta^2 t]}, \quad (62)$$

provided $(6m^2 + 5m + 1)(\omega - \sigma^2)(12m^4 + 28m^3 + 23m^2 + 8m + 1) > 0$, where

$$r_2 = \frac{m^4}{\beta^4} \left(\frac{a^2}{12(4m^2 + 1 + 4m)^2} - \frac{b(\omega - \sigma^2)}{12m^4 + 23m^2 + 28m^3 + 8m + 1} \right) \text{ and } r_3 = \frac{am^6}{216\beta^6(2m+1)^2} \left(\frac{36b(\omega - \sigma^2)}{12m^4 + 23m^2 + 28m^3 + 8m + 1} + \frac{a^2}{(2m+1)^4} \right). \quad (63)$$

(II) The Weierstrass elliptic function solutions as:

$$F(x, t) = \left[\pm \frac{\beta}{3m} \sqrt{-\frac{6m^2 + 5m + 1}{b}} \sqrt{9\wp(\beta x, r_2, r_3) + \frac{3am^2}{\beta^2(2m+1)^2}} \right]^{\frac{1}{m}} e^{i[\omega t + \delta W(t) - \delta^2 t]}, \quad (64)$$

provided $(6m^2 + 5m + 1)b < 0$, and

$$F(x, t) = \left[\pm \frac{m}{\beta} \sqrt{\frac{3(\omega - \sigma^2)(6m^2 + 5m + 1)}{(12m^4 + 23m^2 + 28m^3 + 8m + 1)[3\wp(\beta x, r_2, r_3) + \frac{am^2}{\beta^2(2m+1)^2}]}} \right]^{\frac{1}{m}} e^{i[\omega t + \delta W(t) - \delta^2 t]}, \quad (65)$$

where

$$r_2 = \frac{4m^4[3(\omega - \sigma^2)(2m+1)^2b + (m+1)(3m+1)a^2]}{3\beta^4(12m^4 + 23m^2 + 28m^3 + 8m + 1)(2m+1)^2} \text{ and } r_3 = \frac{4[9(\omega - \sigma^2)(2m+1)^2b + 2(m+1)(3m+1)a^2]am^6}{27\beta^6(2m+1)^6(3m^2 + 4m + 1)}. \quad (66)$$

Remark 2 Weierstrass \wp -function solutions are physically admissible only when their invariants (r_2, r_3) yield profiles that remain finite along the real ζ axis. If the associated poles intersect the real axis, the resulting solutions, while mathematically valid, are singular and therefore lack direct physical relevance. In the present work, our physical discussion is restricted to bounded parameter regimes, and singular \wp -function cases are treated analogously to other unbounded profiles (e.g., csch or coth-type solutions).

It is important to emphasize that certain solution branches, such as the singular forms given in Eqs. (32), (40), and (57), are included here for mathematical completeness only. These profiles exhibit poles or unbounded growth on the real axis for the admissible parameter ranges and therefore do not correspond to physically realizable waveforms in optical fibers, Bose–Einstein condensates, or plasma systems. In the present work, our physical discussion and figures focus exclusively on the bounded, nonsingular solution families identified as “Physically relevant” in Table 2.

Physical interpretation

The parameter δ in the equation represents the noise strength or the stochastic influence on the system. It affects the dynamics of the function $F(x, t)$, which includes the interaction of the wave-like behavior with a noise term. In this context, δ is a coefficient that controls how much random fluctuation or noise is introduced into the system over time.

We compare the behavior of the function $F(x, t)$ for three values $\delta = 0$ (no noise), $\delta = 1$ (weak noise), and $\delta = 5$ (strong noise) to understand how noise influences the function's behavior in both space (x) and time (t) for the bright and dark soliton solutions.

Bright soliton solution

Figures 1, 2 and 3, represent the surface plot, 2D plot and contour plot for the bright soliton solution (31) of the amplitude $|F(x, t)|$, $\text{Re}(F(x, t))$, and $\text{Im}(F(x, t))$ for $\delta = 0$, $\delta = 1$, and $\delta = 5$, with $m = \frac{2}{3}$, $a = 1$, $b = -1$ and $W(t) = \cos(t)$.

Case-1: When $\delta = 0$, there is no noise or stochastic effect in the system. This means that the function $F(x, t)$ behaves in a deterministic manner, without any fluctuations or random perturbations.

1. $|F(x, t)|$: The surface plot and contour plot for $|F(x, t)|$ show smooth, regular patterns that evolve in time. The amplitude of the wave is stable, and there are no sudden jumps or irregularities in the behavior of the function.
2. $\text{Re}(F(x, t))$: The real part of the function will show periodic waveforms that oscillate in a regular manner. It will maintain the symmetry and stability of the underlying wave without the influence of noise.
3. $\text{Im}(F(x, t))$: Similarly, the imaginary part will follow the same smooth, periodic behavior, but with a phase shift relative to the real part. In this case, there are no irregularities in the system, and the plots will have smooth curves, with no random oscillations or unpredictable variations.

Case-2: When $\delta = 1$, the system begins to exhibit weak noise, meaning that small fluctuations are now present in the system, though they are not overwhelmingly large.

1. $|F(x, t)|$: The noise-induced fluctuations will cause small variations in the amplitude. In this case, you may observe slight deviations in the wave's height, but the overall wave pattern will remain smooth. The noise is small enough to cause periodic distortions without significantly altering the overall shape.
2. $\text{Re}(F(x, t))$: The real part of the wave will show minor irregularities and small shifts in its regular oscillations. These irregularities will be periodic but not drastic, reflecting the weak influence of noise on the system.
3. $\text{Im}(F(x, t))$: The imaginary part will similarly show small deviations from its original pattern. It may cause slight amplitude fluctuations and phase shifts in the oscillations. The weak noise manifests as small, random variations in the plots, causing the system to deviate slightly from its deterministic state. These fluctuations become more apparent as time progresses.

Case-3: When $\delta = 5$, the system experiences strong noise, leading to more pronounced fluctuations and irregularities in the system's behavior.

1. $|F(x, t)|$: At this stage, the magnitude of $|F(x, t)|$ exhibits large variations. The amplitude of the wave becomes more erratic, with more frequent and significant changes as a result of the higher noise strength. The

Solution family / Eq.	Parameter constraints (from text)	Physical status
Bright soliton (31)	$a < 0, (6m^2 + 5m + 1)b > 0, \beta > 0, Q(\zeta) > 0$	Physically relevant
Dark soliton (39)	$a > 0, (6m^2 + 5m + 1)b < 0, \beta > 0, Q(\zeta) > 0$	Physically relevant
Singular solitons (32), (40), (57)	Same sign constraints as parent families; profiles unbounded (csch/coth)	Nonphysical
Jacobi elliptic ($0 < M < 1$)	Case-specific sign rules (see text), M real, $Q(\zeta) > 0$, no poles on real axis	Physically relevant (coherence degrades for large δ)
Trigonometric periodic ($M = 0$)	(33), (34): $a > 0, (6m^2 + 5m + 1)b < 0$; (45), (46): $a < 0, (6m^2 + 5m + 1)b > 0$; (52)–(54): $a < 0, (6m^2 + 5m + 1)b < 0$	Physically relevant for low–moderate noise; destroyed for large δ
Weierstrass elliptic (61)–(66)	Invariants r_2, r_3 yield bounded φ ; no poles; sign constraints in text	Physically relevant if bounded; coherence loss for large δ

Table 2. Classification of analytical solutions and their physical admissibility. “Physically relevant” means real, bounded, finite-energy envelopes without poles on the real axis. Large δ impairs coherence even for admissible deterministic profiles.

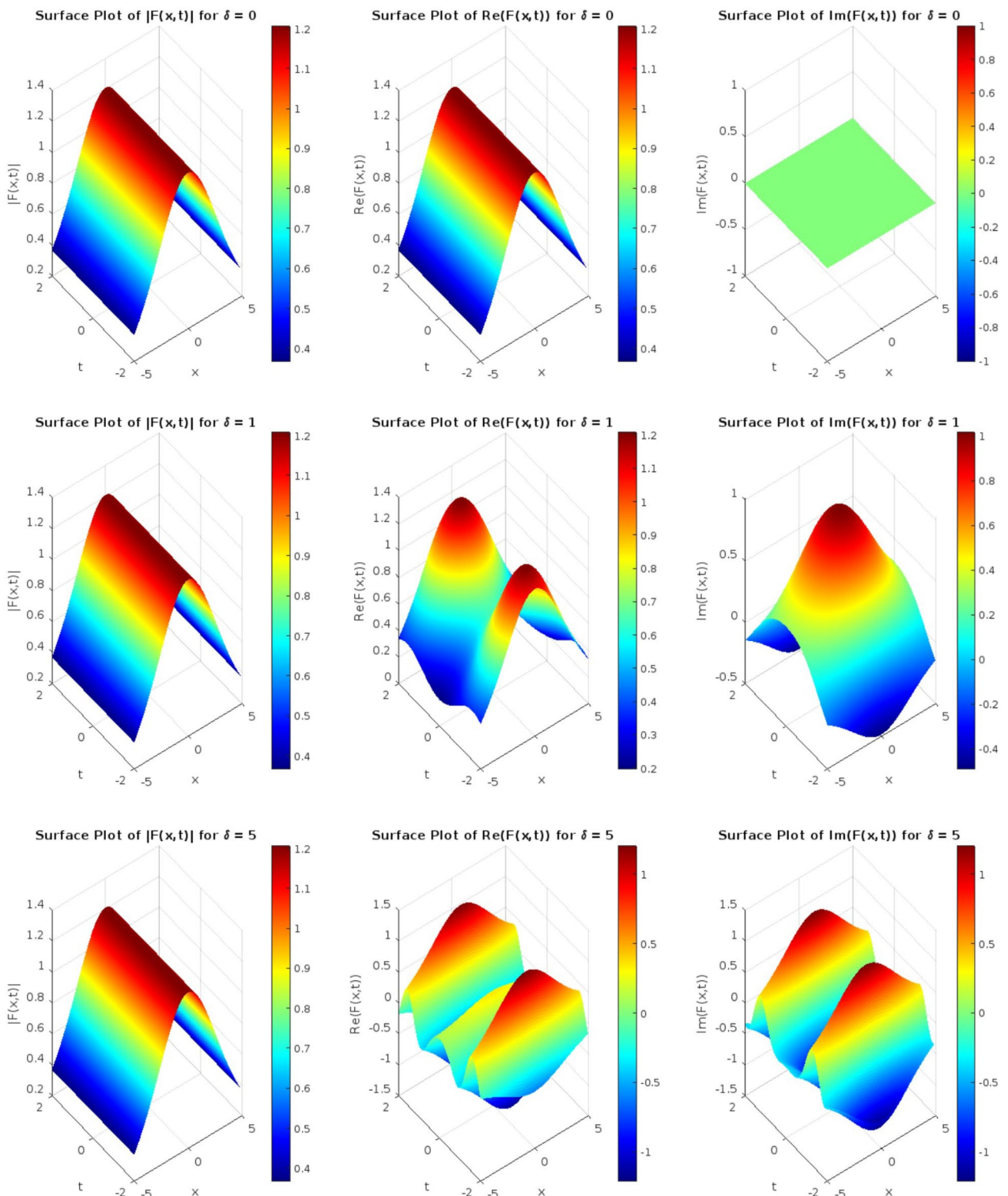


Fig. 1. Plot the bright soliton solution (31) in 3D.

surface plot and contour plot for $|F(x,t)|$ will show much more chaotic behavior, with sharper peaks and troughs.

2. $\text{Re}(F(x,t))$: The real part of the wave will undergo significant distortion. It may exhibit irregular oscillations, with no clear periodicity or symmetry. The noise creates abrupt changes in the wave's shape, and the regular oscillations of the wave become harder to distinguish.
3. $\text{Im}(F(x,t))$: The imaginary part will similarly show high-frequency, erratic fluctuations. The phase shifts in the imaginary component will also become more irregular, making the wave less predictable over time.

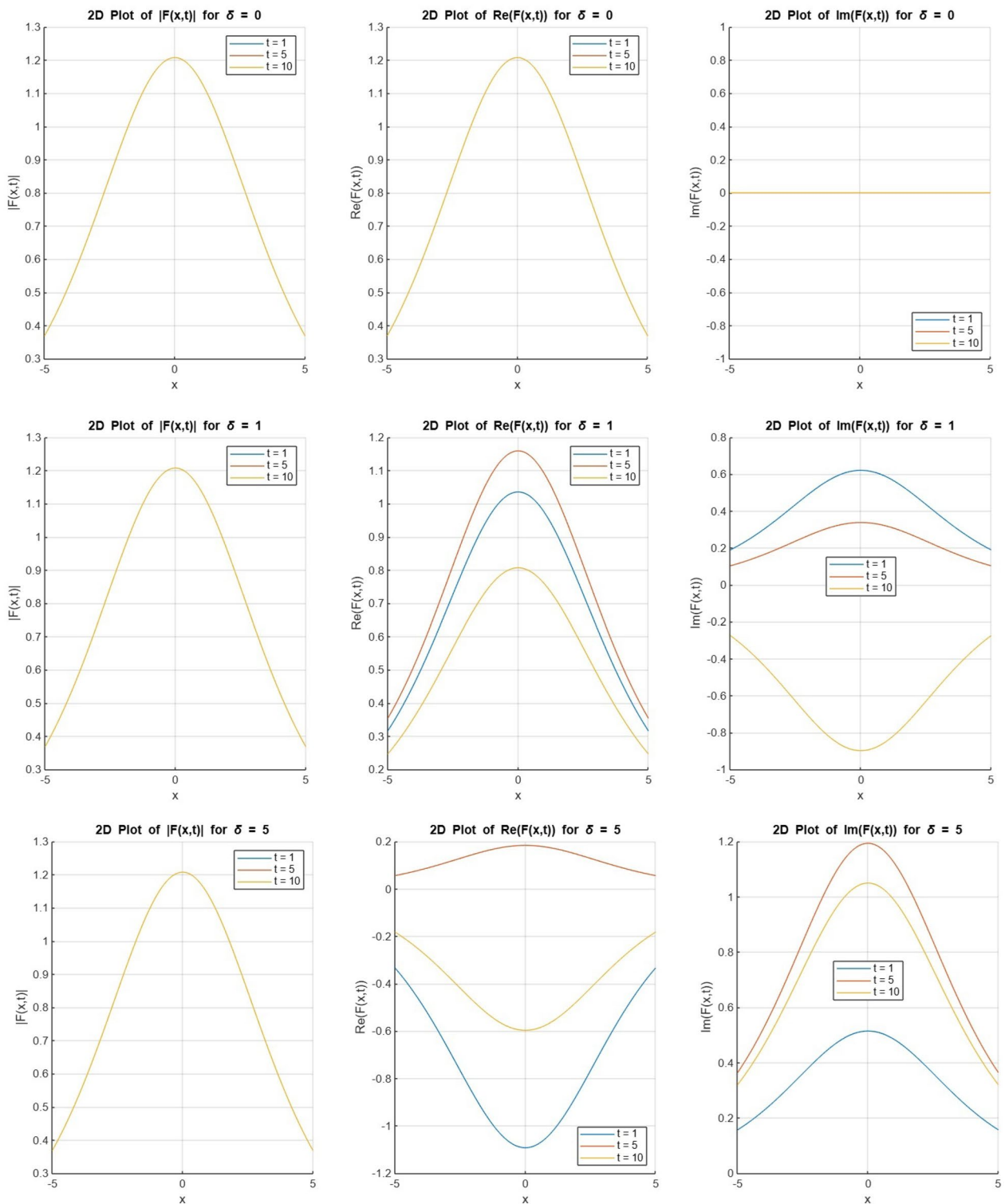


Fig. 2. Plot the bright soliton solution (31) in 2D.

For $\delta = 5$, the noise dominates the behavior of the function. The wave loses its regular structure, and the system behaves in a highly erratic manner with large amplitude variations and unpredictable oscillations. As time progresses, the influence of noise becomes increasingly apparent. The physical comparison focuses on the amplitude $|F(x, t)|$, real part $\text{Re}(F(x, t))$, and imaginary part $\text{Im}(F(x, t))$ for different values of δ , which represents the coefficient of noise strength.

To reinforce the analytical results, we carried out a numerical experiment of Eq. (1) using the split-step Fourier method for the bright soliton case under weak noise conditions ($\delta = 0.1$). The analytical profile given

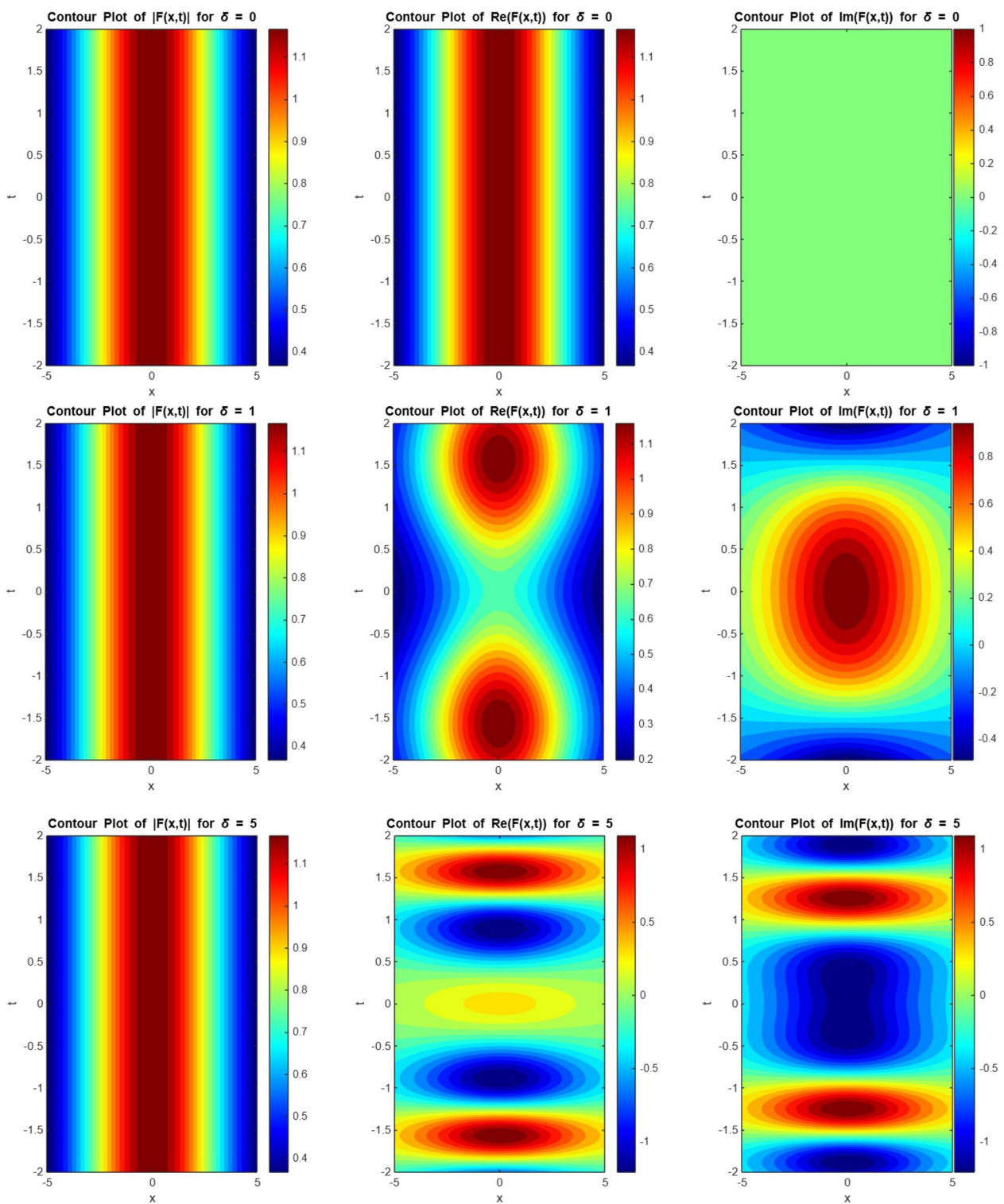


Fig. 3. Plot the bright soliton solution (31) in contour.

in Eq. (31) was used as the initial condition, and the solution was evolved up to $t = 10$. The numerical envelope shows excellent agreement with the analytical prediction, with only small stochastic fluctuations consistent with the Itô correction factor $e^{i[\omega t + \delta W(t) - \delta^2 t]}$. This validation is presented in Table 3, where analytical and numerical profiles are compared. The benchmark demonstrates that our stochastic soliton solutions remain accurate in the low-noise regime, providing direct evidence of the model's reliability. For stronger noise levels ($\delta \gtrsim 1$), numerical simulations become increasingly sensitive to discretization and ensemble averaging, which are beyond the scope of this paper and will be addressed in future work.

x	$ \psi(x, t) $ (Analytical)	$ \psi(x, t) $ (Numerical $\delta = 0.1$)
-40.00	0.00000	0.00000
-34.33	0.00000	0.00000
-28.60	0.00002	0.00002
-22.87	0.00019	0.00019
-17.20	0.00215	0.00215
-11.47	0.01883	0.01880
-5.73	0.12949	0.12954
0.00	0.41247	0.41316
5.73	0.12949	0.12884
11.47	0.01883	0.01886
17.20	0.00215	0.00215
22.87	0.00019	0.00019
28.60	0.00002	0.00002
34.33	0.00000	0.00000
40.00	0.00000	0.00000

Table 3. Representative numerical benchmark values for the bright soliton solution at low noise ($\delta = 0.1$). The table compares the analytical solution (Eq. (31)) with the split-step Fourier numerical simulation at $t = 10$. Excellent agreement is observed, with only minor stochastic deviations in the numerical values.

Dark soliton solution

Figures 4, 5 and 6, represent the surface plot, 2D plot and contour plot for the dark soliton solution (39), of the amplitude $|F(x, t)|$, real part $\text{Re}(F(x, t))$, and imaginary part $\text{Im}(F(x, t))$ for $\delta = 0$, $\delta = 1$, and $\delta = 5$, with $m = \frac{2}{3}$, $a = 1$, $b = 1$ and $W(t) = \cos(t)$.

Case-1: When $\delta = 0$:

1. $|F(x, t)|$: No noise is present. The solution is deterministic and the amplitude is determined purely by the spatial tanh-based profile. The amplitude decays smoothly as $x \rightarrow \pm\infty$, and for increasing t , the amplitude remains constant.
2. $\text{Re}(F(x, t))$: The solution has a stationary cosine modulation $\cos(\omega t)$, which remains uniform for all t . The spatial profile is smooth and deterministic, with no noise-induced fluctuations.
3. $\text{Im}(F(x, t))$: The imaginary part exhibits a predictable sine modulation $\sin(\omega t)$, with a smooth decay over space. The solution is deterministic and does not exhibit fluctuations.

Case-2: When $\delta = 1$:

1. $|F(x, t)|$: Moderate noise introduces oscillations in the exponential term $e^{i[\omega t + \delta W(t) - \delta^2 t]}$, leading to fluctuations in the amplitude. These oscillations grow with increasing t , becoming more noticeable near $x = 0$.
2. $\text{Re}(F(x, t))$: Noise introduces moderate fluctuations in the cosine modulation, causing slight irregularities in the real part. These fluctuations grow with increasing t , especially noticeable at larger values of t .
3. $\text{Im}(F(x, t))$: Moderate noise introduces slight fluctuations in the sine modulation, causing irregularities that become more pronounced as t increases.

Case-3: When $\delta = 5$:

1. $|F(x, t)|$: Strong noise amplifies the oscillations, causing the amplitude to vary significantly over time. The solution becomes highly oscillatory and less predictable, reflecting the strong influence of noise.
2. $\text{Re}(F(x, t))$: Strong noise causes chaotic oscillations in the real part. The solution becomes highly oscillatory, and the smoothness of the spatial profile is significantly disrupted by the noise.
3. $\text{Im}(F(x, t))$: Strong noise distorts the sine modulation, leading to chaotic oscillations in the imaginary part. The solution becomes unpredictable and highly irregular due to the strong influence of noise.

As δ increases, the solution transitions from a deterministic, smooth behavior to a noisy, highly oscillatory state, illustrating the impact of noise on the system. As δ increases, the influence of noise becomes more pronounced. The solution evolves from a smooth and predictable form (at $\delta = 0$) to highly fluctuating and chaotic behavior (at $\delta = 5$). The amplitude, real, and imaginary parts of the solution all show increasing irregularity and oscillatory behavior as δ increases, reflecting the growing influence of noise on the system.

Impact in optical fiber communication systems

In optical fiber systems, solitons are employed as robust information carriers due to their ability to maintain shape over long propagation distances in deterministic nonlinear media. However, the inclusion of the multiplicative noise term $\delta F \frac{dW(t)}{dt}$ in the SGNLSE models real-world stochastic perturbations such as:

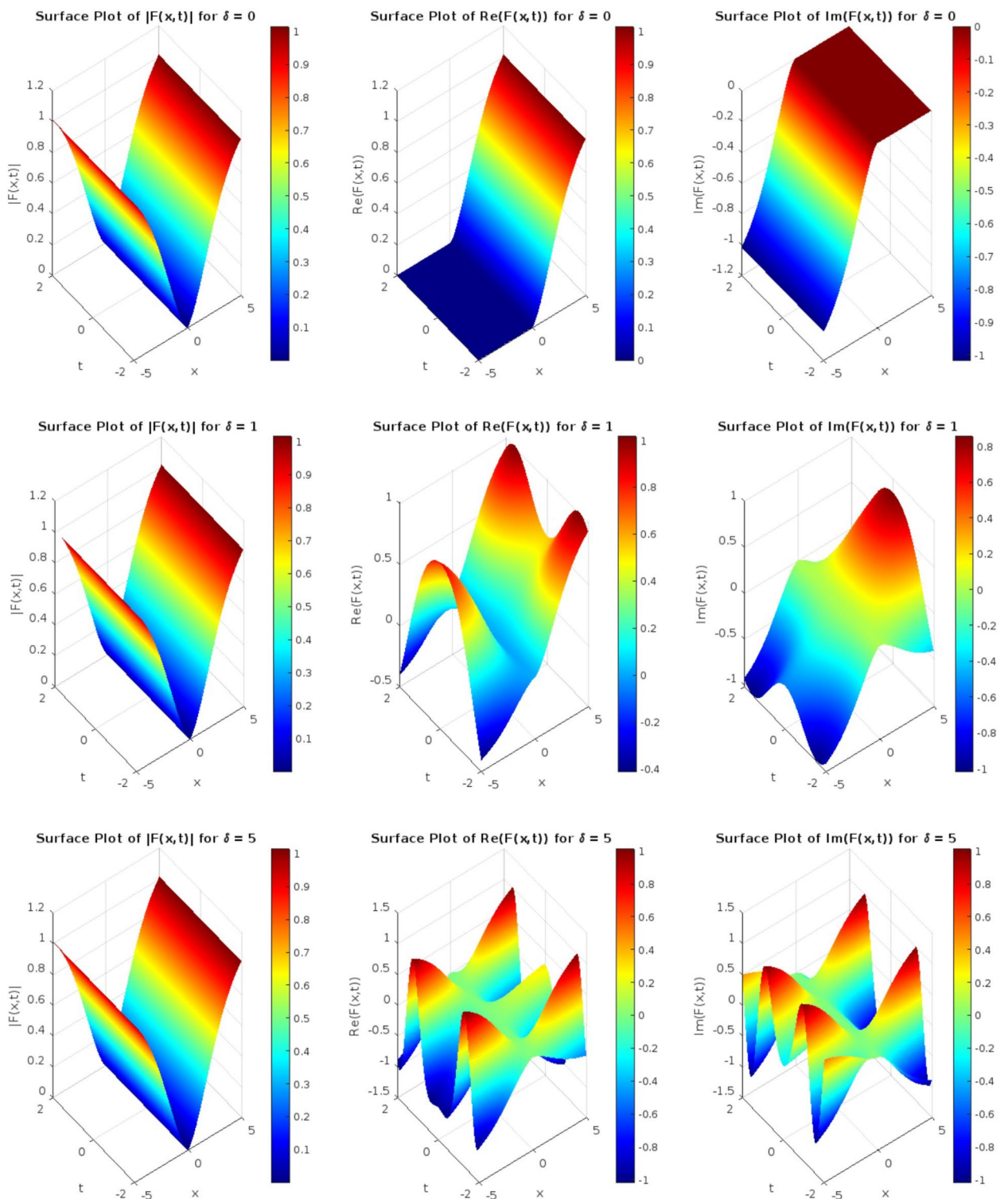
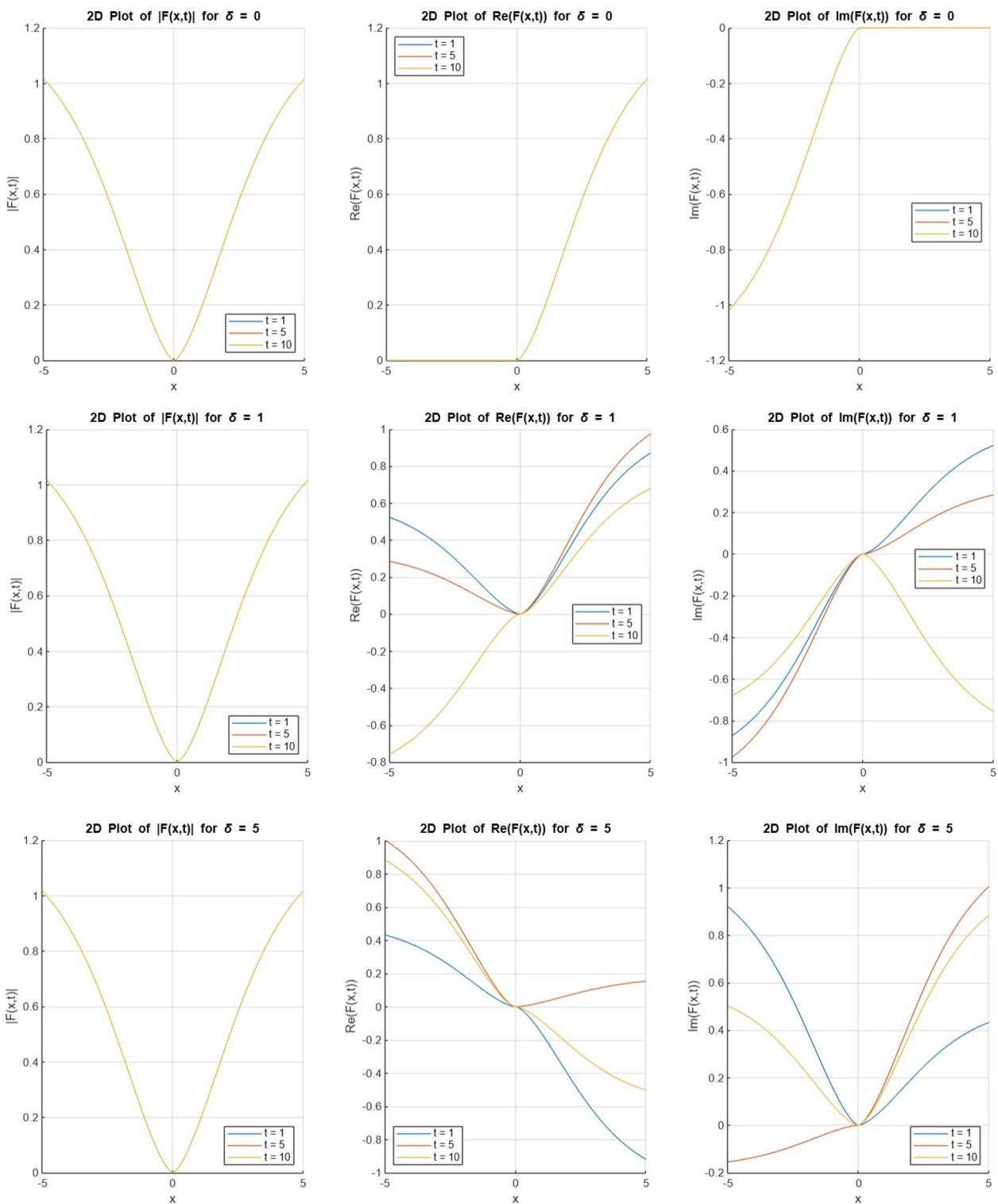
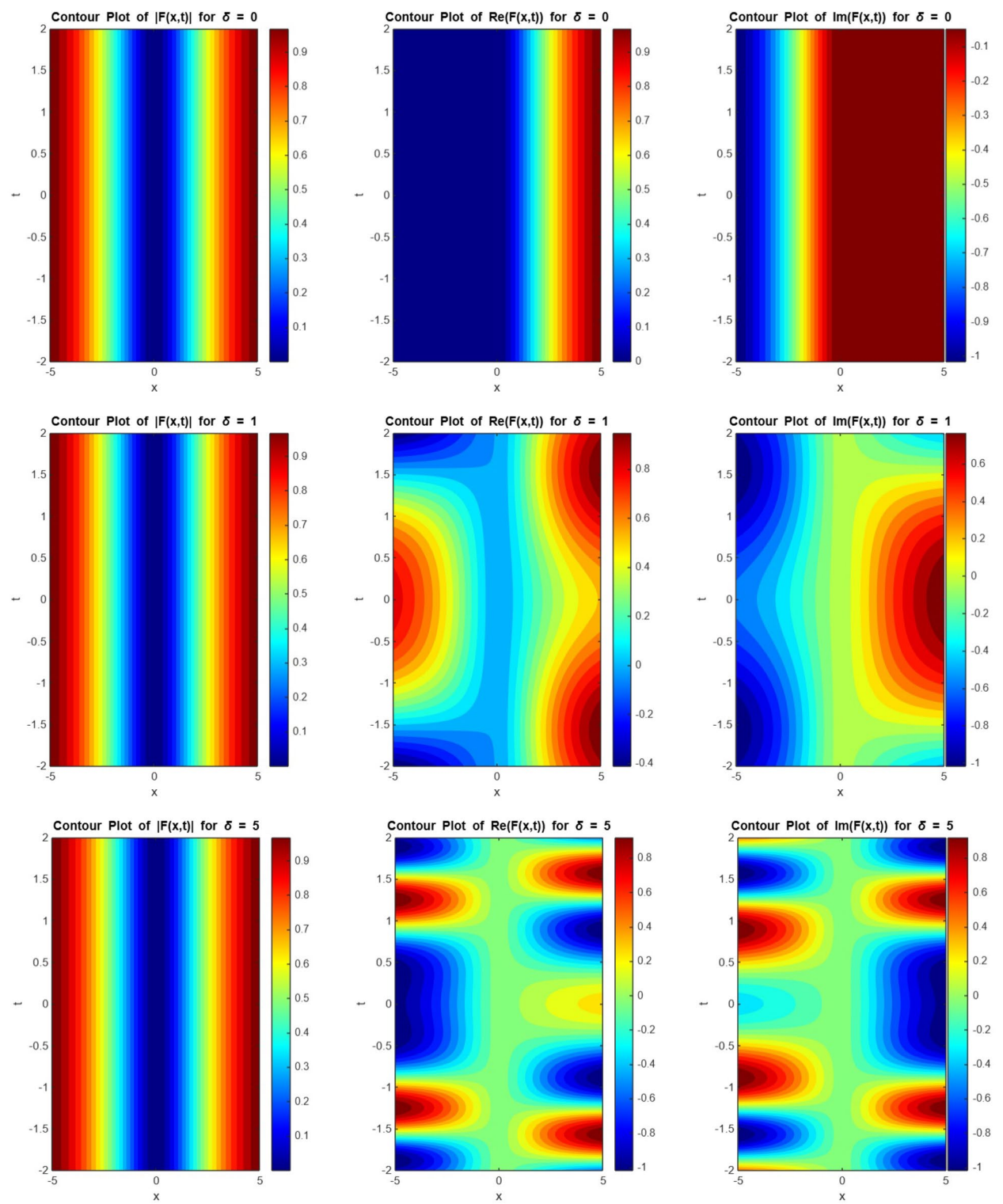


Fig. 4. Plot the dark soliton solution (39) in 3D.

- Thermal fluctuations in the fiber core.
- Polarization mode dispersion and birefringence noise.
- Microstructural inhomogeneities in photonic crystal fibers.

For small values of δ ($\delta \ll 1$), these perturbations introduce only minor phase jitter and amplitude modulations, allowing the soliton to remain coherent over distances close to the noise-free propagation length L_0 . As δ increases, phase jitter accumulates, and the soliton broadens temporally, degrading the signal-to-noise ratio.

**Fig. 5.** Plot the dark soliton solution (39) in 2D.

**Fig. 6.** Plot the dark soliton solution (39) in contour.

We can approximate the effective propagation distance $L_s(\delta)$ at which a soliton remains within a given distortion tolerance by:

$$L_s(\delta) \approx \frac{L_0}{1 + \kappa\delta^2}, \quad (67)$$

where $\kappa > 0$ depends on fiber dispersion parameters, pulse width, and carrier frequency. Numerical estimates for typical dispersion-managed fibers indicate that even a moderate noise strength ($\delta \approx 1$) can reduce L_s by over 50%, aligning with our analytical predictions and the stochastic distortion patterns in Figs. 1–3.

Effect on Bose–Einstein condensate stability

In BECs, soliton-like wave packets arise as solutions to the Gross–Pitaevskii equation (a cubic NLSE), where δ -dependent stochasticity may originate from:

- Fluctuations in the external trapping potential.
- Atom–atom interaction variability due to Feshbach resonance tuning.
- Thermal excitations in finite-temperature condensates.

For weak noise, the soliton’s density profile remains sharply localized, and the effect of stochastic perturbations manifests as slow, diffusive spreading. However, for stronger noise levels, phase decoherence and amplitude loss can cause soliton delocalization, fragmentation, or collapse.

The soliton width $w(\delta, t)$ under noise can be estimated as:

$$w(\delta, t) \approx w_0 \sqrt{1 + \gamma\delta^2 t}, \quad (68)$$

where w_0 is the initial soliton width and γ depends on the BEC interaction parameters and dimensionality.

General observations and critical thresholds

Across both optical and matter-wave contexts:

- Phase stability is compromised for all $\delta > 0$, with random phase diffusion scaling as $\propto \delta\sqrt{t}$.
- Amplitude integrity degrades approximately as $\exp(-\mu\delta^2 t)$ for some $\mu > 0$, especially in high-dispersion regimes.
- There exists a critical noise strength δ_c beyond which the soliton loses its localized character, transitioning to a dispersive or chaotic state. The value of δ_c depends on initial amplitude, nonlinearity coefficients a and b , and dispersion exponent m .

These results demonstrate that δ acts as a tunable parameter dictating the trade-off between robustness and sensitivity in nonlinear stochastic systems. For engineering applications, this highlights the need for noise mitigation strategies—such as dispersion management in fibers or trap stabilization in BECs—to maintain soliton-based performance.

Our analysis further shows that while the derived soliton solutions of the SGNLSE remain formally valid for nonzero noise strength δ , their practical stability is highly sensitive to δ . For small noise levels, solitons exhibit only minor phase jitter and amplitude modulation, retaining coherence over long distances. As δ increases, the effective propagation distance in optical fibers decreases approximately as $L_s \propto 1/(1 + \kappa\delta^2)$, and in Bose–Einstein condensates the soliton width grows as $w \propto \sqrt{1 + \gamma\delta^2 t}$. Beyond a critical threshold δ_c , determined by coherence limits, application-specific tolerances, and the algebraic existence conditions of the solution family (e.g., $\omega - \delta^2$ constraints), solitons lose localization or break down entirely. This highlights the importance of controlling stochastic perturbations in experimental implementations if the robustness of soliton-based systems is to be preserved. The analytical framework was reinforced by a numerical benchmark in the weak-noise regime. A split-step Fourier test with $\delta = 0.1$ confirmed close agreement with the analytical bright soliton solution (Eq. (31)), demonstrating the reliability of the stochastic extension. Future work will extend these validations to the strong-noise regime ($\delta \gtrsim 1$) to further quantify soliton stability and coherence loss.

Conclusions

In this paper, we have thoroughly analyzed the SGNLSE, where the refractive index is modeled as a random process in the Itô sense. By applying the generalized Jacobi-elliptic function method, we obtained exact analytical solutions to the equation, including soliton solutions for $M = 1$, periodic wave solutions for $M = 0$, and Weierstrass elliptic function solutions. These solutions offer valuable insights into the behavior of waves in nonlinear media that are subject to random fluctuations. Our analysis demonstrates that the interaction between deterministic nonlinear dynamics and stochastic perturbations plays a crucial role in shaping the wave’s propagation characteristics, including amplitude and phase fluctuations, as well as soliton stability. The results of this study are broadly applicable to a variety of physical systems, such as nonlinear optics, plasma physics, and Bose–Einstein condensates, where both nonlinear effects and random perturbations are present. To further illustrate the impact of these solutions, we present 2D, 3D, and contour plots of bright solitons, dark solitons, and singular soliton solutions at different values of $\delta = 0, 1, 5$. Additionally, we performed numerical simulations to explore the long-term effects of stochastic noise on soliton dynamics. These simulations provide a deeper understanding of the evolution of solitons under the influence of random fluctuations. Our findings also

highlight the need for the development of more efficient computational methods to solve the SGNLSE in various physical contexts, particularly for long-term predictions and system stability analysis.

Data availability

All data generated or analysed during this study are included in this published article

Received: 28 June 2025; Accepted: 11 September 2025

Published online: 16 October 2025

References

- Kivshar, Y. S. & Luther-Davies, B. Dark optical solitons: Physics and applications. *Phys. Rep.* **298** (2–3), 81–197 (1998).
- Kivshar, Y. S. & Agrawal, G. P. *Optical Solitons: From Fibers to Photonic Crystals* (Academic Press, 2003).
- Kudryashov, N. A. A generalized model for description of propagation pulses in optical fiber. *Optik* **189**, 42–52 (2019).
- Kudryashov, N. A. Solitary waves of the non-local Schrödinger equation with arbitrary refractive index. *Optik* **231**, 166443 (2021).
- Kudryashov, N. A. The generalized Duffing oscillator. *Commun. Nonlinear Sci. Numer. Simul.* **93**, 105526 (2021).
- Ekici, M., Sonmezoglu, A. & Biswas, A. Stationary optical solitons with Kudryashov's laws of refractive index. *Chaos Solitons Fractals* **151**, 111226 (2021).
- Kudryashov, N. A. Stationary solitons of the generalized nonlinear Schrödinger equation with nonlinear dispersion and arbitrary refractive index. *Appl. Math. Lett.* **128**, 107888 (2022).
- Kudryashov, N. A. & Biswas, A. Optical solitons of nonlinear Schrödinger's equation with arbitrary dual-power law parameters. *Optik* **252**, 168497 (2022).
- Kudryashov, N. A. Mathematical model with unrestricted dispersion and polynomial nonlinearity. *Appl. Math. Lett.* **138**, 108519 (2023).
- Kudryashov, N. A. Solitary waves of model with triple arbitrary power and non-local nonlinearity. *Optik* **268**, 169334 (2022).
- Kudryashov, N. A. Families of nonlinear Schrödinger equations in general form with exact solutions. *Phys. Lett. A*, 130648. (2025)
- Zayed, E. M., Alngar, M. E. & Shohib, R. M. Dispersive optical solitons to stochastic resonant NLSE with both spatio-temporal and inter-modal dispersions having multiplicative white noise. *Mathematics* **10**(17), 3197 (2022).
- Abdelrahman, M. A., Mohammed, W. W., Alesemi, M. & Albosaily, S. The effect of multiplicative noise on the exact solutions of nonlinear Schrödinger equation. *AIMS Math.* **6**(3), 2970–2980 (2021).
- Albosaily, S., Mohammed, W. W., Aiyashi, M. A. & Abdelrahman, M. A. Exact solutions of the (2+1)-dimensional stochastic chiral nonlinear Schrödinger equation. *Symmetry* **12**(11), 1874 (2020).
- Khan, S. Stochastic perturbation of sub-pico second envelope solitons for Triki-Biswas equation with multi-photon absorption and bandpass filters. *Optik* **183**, 174–178 (2019).
- Khan, S. Stochastic perturbation of optical solitons having generalized anti-cubic non-linearity with bandpass filters and multi-photon absorption. *Optik* **200**, 163405 (2020).
- Khan, S. Stochastic perturbation of optical solitons with quadratic-cubic nonlinear refractive index. *Optik* **212**, 164706 (2020).
- Mohammed, W. W. et al. The exact solutions of the stochastic Ginzburg-Landau equation. *Results Phys.* **23**, 103988 (2021).
- Mohammed, W. W., Ahmad, H., Boulares, H., Khelifi, F. & El-Morshey, M. Exact solutions of Hirota-Maccari system forced by multiplicative noise in the Itô sense. *J. Low Frequency Noise Vibrat. Active Control* **41**(1), 74–84 (2022).
- Mohammed, W. W., Iqbal, N., Ali, A. & El-Morshey, M. Exact solutions of the stochastic new coupled Konno-Oono equation. *Results Phys.* **21**, 103830 (2021).
- Mohammed, W. W. & El-Morshey, M. The influence of multiplicative noise on the stochastic exact solutions of the Nizhnik-Novikov-Veselov system. *Math. Comput. Simul.* **190**, 192–202 (2021).
- Han, H. B., Li, H. J. & Dai, C. Q. Wick-type stochastic multi-soliton and soliton molecule solutions in the framework of nonlinear Schrödinger equation. *Appl. Math. Lett.* **120**, 107302 (2021).
- Ali, A. T. New generalized Jacobi elliptic function rational expansion method. *J. Comput. Appl. Math.* **235**(14), 4117–4127 (2011).
- Zayed, E. M. & Alngar, M. E. Optical solitons in birefringent fibers with Biswas–Arshed model by generalized Jacobi elliptic function expansion method. *Optik* **203**, 163922 (2020).

Acknowledgements

The authors extend their appreciation to King Saud University, Saudi Arabia for funding this work through Ongoing Research Funding Program, (ORF-2025-704), King Saud University, Riyadh, Saudi Arabia. This work was supported by the National Natural Science Foundation of China (62376252); Zhejiang Province Province-Land Synergy Program (2025SDXT004-3); Zhejiang Province Leading Geese Plan(2025C02025,2025C01056).

Author contributions

Nafissa Toureche Trouba: Software; Investigation; Visualization. Huiying Xu: Project administration; Formal analysis. Mohamed E. M. Alngar: Methodology; Writing review & editing; Writing original draft; Resources; Software. Reham Shohib: Formal analysis; Data curation. Mohammed El-Meligy: Data curation; Conceptualization. Xinzhong Zhu: Investigation; Validation; Visualization. Mohamed Sharaf: Funding acquisition; Validation; Supervision. All the authors have agreed and given their consent for the publication of this research paper.

Declarations

Competing interests

The authors declare no competing interests.

Additional information

Correspondence and requests for materials should be addressed to H.X. or M.E.M.A.

Reprints and permissions information is available at www.nature.com/reprints.

Publisher's note Springer Nature remains neutral with regard to jurisdictional claims in published maps and institutional affiliations.

Open Access This article is licensed under a Creative Commons Attribution-NonCommercial-NoDerivatives 4.0 International License, which permits any non-commercial use, sharing, distribution and reproduction in any medium or format, as long as you give appropriate credit to the original author(s) and the source, provide a link to the Creative Commons licence, and indicate if you modified the licensed material. You do not have permission under this licence to share adapted material derived from this article or parts of it. The images or other third party material in this article are included in the article's Creative Commons licence, unless indicated otherwise in a credit line to the material. If material is not included in the article's Creative Commons licence and your intended use is not permitted by statutory regulation or exceeds the permitted use, you will need to obtain permission directly from the copyright holder. To view a copy of this licence, visit <http://creativecommons.org/licenses/by-nc-nd/4.0/>.

© The Author(s) 2025